VECTOR FIELD TOPOLOGY WITH CLIFFORD ALGEBRA

Gerik Scheuermann and Hans Hagen
Computer Science Department, University of Kaiserslautern
P. O. Box 30 49, 67653 Kaiserlautern, Germany
{scheuer,hagen}@informatik.uni-kl.de

Heinz Krüger
Physics Department, University of Kaiserslautern
P. O. Box 30 49, 67653 Kaiserlautern, Germany
krueger@physik.uni-kl.de

Abstract

One way to visualize vector fields was based on their qualitative structure by showing the field topology after linear or bilinear interpolation. This paper extends this to cases of nonlinear behavior in the grid cells. It uses new ideas about the analysis of some polynomial vector fields which have been proved by using Clifford algebra and analysis. They are used as local model for the visualization and allow general positions and arbitrary Poincare indices of the critical points in the interesting regions.

1 INTRODUCTION

There is a growing interest in vector field visualization based on topology in the last years ([Helm91], [Glob91]). But all methods so far begin with linear or bilinear interpolation of the grid data and start the analysis of the topology from there. This is a fast algorithm and one receives good results as long as the critical points are well separated and of simple type. But this is often not the case and then the linear or bilinear interpolation of the grid cells reduces artificially the possible topological structures, especially it makes the existence of critical points of index higher than 1 or lower than -1 impossible.

One problem is that in the literature ([Arno91], [Guck83], [Hirs74]) one finds an analysis of linear fields and some special equations, where the position, number and type of critical points is not arbitrary. The reason is that it is difficult to analyse non-linear fields in the classical way by finding solutions for the integral curves.

This drawback caused us to look for different ways to analyse the topology. The starting point is to change the coordinates and use the geometric insights provided by Clifford algebra to prove results about the relation between algebraic description and topology.

Our paper continues with some topological background on the relation between vector field topology and surface topology which are connected by the Poincare indices of the critical points and the Euler charcteristic of the surface. Clifford algebra and analysis are described in section 3 and used to obtain the desired results about the topology of polynomial vector fields in Section 4. The last section gives an overview over the algorithm and includes an example.

Typical applications of this approach are the magnetic fields inside coils or transformers. Several windings construct critical points of higher index. The eddy motions in turbulent flows are also a source for higher order critical points.

2 TOPOLOGICAL REMARKS

This section introduces the concepts of the Euler characteristic of a topological space and the Poincaré index of a zero of a vector field and their relation by the Poincaré-Hopf theorem.

A topological space X homeomorphic to the interior $\dot{D}^n$ of the unit disc is called a **n-cell**.

A **cellular decomposition** of a Hausdorff space X is a set of subspaces of X with the following properties

(i) $X = \bigcup_{e \in C}$ and $e \cap e' = \emptyset$ for $e \neq e'$

(ii) Every $e \in C$ is a $|e|$-cell, $|e| \in R$.

(iii) For each $e \in C$ exists a map $\phi_e : D^n \to X$, $n = |e|$, so that $\phi_e|\dot{D}^n$ is a homeomorphism of $\dot{D}^n$ and e and $\phi_e(S^{n-1}) \subset X^{n-1} := \bigcup_{e' \in C, |e'| \leq n-1} e'$.

X^{n-1} is called **$(n-1)$-skeleton** of the cellular decomposition.

Such a cellular decomposition is called **CW-decomposition** if

(C) for every $e \in C$ is $\bar{e}$ a subset of a finite union of cells in C. (**closure finite**)

(W) A subset $A \subset X$ is closed if and only if $A \cap \bar{e}$ is closed in $\bar{e}$ $\forall e \in C$. (**weak topology**)

A **CW-space** consists of a pair (X,C) of a Hausdorff space X and a CW-decomposition C.

Definition 1 *Let (X,C) be a finite CW-space and let α_n be the number of n-cells in C. The* **Euler characteristic** $\chi(X)$ *of X is*

$$\chi(X) = \sum_{q=0}^{\infty} (-1)^q \alpha_q \tag{1}$$

Definition 2 *Let M, N be oriented n-manifolds and let M be compact, N connected. Further let $f : M \to N$ be a smooth map with regular point $x \in M$, so that $T_x f : T_x M \to T_{f(x)} N$ is a linear isomorphism between oriented vector spaces. Define the* **sign$(T_x f)$** *of $T_x f$ to be $+1$ or -1 according as $T_x f$ preserves or reverses orientation. For a regular value $y \in N$ the* **Brouwer degree** *is defined by*

$$\deg(f; y) := \sum_{x \in f^{-1}(y)} sign(T_x f) \tag{2}$$

Definition 3 *Let M be a compact, connected m-manifold with boundary and $v : M \to TM$ a smooth vector field with isolated zero at $z \in M$. One has a positive oriented chart (ϕ, U), so that $z \in U$ is the only zero of v in U. Further there is a small sphere $S \subset \phi(U)$ centered at $\phi(z)$. With the terms $V := \phi(U)$, $\pi_2 : V \times R^n \to R^n$, $v' : V \to R^n$, $v'(x) = \pi_2 \circ T\phi \circ v \circ \phi^{-1}(x)$, a map $\bar{v} : S \to S^{n-1}$ can be defined by $\bar{v}(x) := \frac{v'(x)}{\|v'(x)\|}$. The Brouwer degree of this map is called* **Poincaré index** *ind_z of v at the zero z.*

A connection between the indices of a vector field and the Euler characteristic of the manifold is given by the following theorem.

Theorem 4 (Poincaré-Hopf) *Let M be a compact oriented n-manifold with boundary and $v : M \to TM$ a smooth vector field with isolated zeros. If $\delta M \neq \emptyset$ then let v(x) be an outward vector for $x \in \delta M$. The sum of the indices at the zeros equals the Euler characteristic of M :*

$$\sum_{\substack{z \in M \\ v(z) = 0}} ind_z = \chi(M) \tag{3}$$

Proof : [Stoe94, p. 35-41] QED.

3 CLIFFORD ALGEBRA

Clifford algebra extends the classical description of an euclidean n-space as a real n-dimensional vector space with scalar product to a real algebra. It gives a way to multiply vectors in arbitrary dimensions and get a geometric interpretation of the result [Hest86]. In our 2D-case it gives a way to describe the relation between real and complex numbers in a nice way.

For the euclidean plane we have a 4-dimensional R-algebra G_2 with the basis $\{1, e_1, e_2, i = e_1 e_2\}$ as a real vector space. The multiplication is defined as associative, bilinear and by the equations

$$1 e_j = e_j \quad j = 1,2 \tag{4}$$

$$e_j e_j = 1 \quad j = 1,2 \tag{5}$$

$$i = e_1 e_2 = -e_2 e_1 \tag{6}$$

The usual vectors $(x, y) \in R^2$ are identified with

$$x e_1 + y e_2 \in E^2 \subset G_2 \tag{7}$$

and the complex numbers $a + bi \in C$ with

$$a1 + bi \in G_2 \tag{8}$$

For a real vector field

$$v : R^2 \rightarrow R^2 \quad (x,y) \mapsto (v_1, v_2) \tag{9}$$

one sets the Clifford vector field

$$v : E^2 \rightarrow E^2 \quad r = xe_1 + ye_2 \mapsto v_1 e_1 + v_2 e_2 \tag{10}$$

The Poincaré-Index can then be defined as

$$ind_a v = \lim_{\epsilon \to 0} \frac{1}{2\pi i} \int_{S^1_\epsilon} \frac{v \wedge dv}{v^2} \tag{11}$$

where

$$a \wedge b = < ab >_2 = \frac{1}{2}(ab - ba) \tag{12}$$

denotes the outer product of Grassmann for $a, b \in E^2$.

4 VECTOR FIELDS IN MEANIGFUL COORDINATES

For our analysis of vector fields it is necessary to look at $v : R^2 \rightarrow R^2 \subset G_2$ in suitable coordinates. Let $z = x + iy$, $\bar{z} = x - iy$ be complex numbers in the algebra. This means

$$x = \frac{1}{2}(z + \bar{z}) \tag{13}$$

$$y = \frac{1}{2i}(z - \bar{z}) \tag{14}$$

We get

$$\begin{aligned} v(r) &= v_1(x,y)e_1 + v_2(x,y)e_2 \\ &= [v_1(\frac{1}{2}(z+\bar{z}), \frac{1}{2i}(z-\bar{z})) - \\ &\quad iv_2(\frac{1}{2}(z+\bar{z}), \frac{1}{2i}(z-\bar{z}))]e_1 \\ &= E(z,\bar{z})e_1 \end{aligned} \tag{15}$$

where

$$\begin{aligned} E : \quad C^2 &\rightarrow C \subset G_2 \\ (z,\bar{z}) &\mapsto v_1(\frac{1}{2}(z+\bar{z}), \frac{1}{2i}(z-\bar{z})) \\ &\quad -iv_2(\frac{1}{2}(z+\bar{z}), \frac{1}{2i}(z-\bar{z})) \end{aligned} \tag{16}$$

is a complex-valued function of two complex variables. The idea is now to analyse E instead of v and get topological results directly from the formulas in some interesting cases.

Let us first assume that E and v are linear.

Theorem 5 *Let*

$$v(r) = (az + b\bar{z} + c)e_1 \tag{17}$$

be a linear vector field. For $|a| \neq |b|$ it has a unique zero at $z_0 e_1 \in R^2$. For $|a| > |b|$ has v one saddle point with index -1. For $|a| < |b|$ it has one critical point with index 1. The special types in this case can be got from the following list :

(1) $Re(b) = 0 \Leftrightarrow$ circle at z_0.

(2) $Re(b) \neq 0$, $|a| > |Im(b)| \Leftrightarrow$ node at z_0.

(3) $Re(b) \neq 0$, $|a| < |Im(b)| \Leftrightarrow$ spiral at z_0.

(4) $Re(b) \neq 0$, $|a| = |Im(b)| \Leftrightarrow$ focus at z_0.

In cases $2) - 4)$ one has a sink for $Re(b) < 0$ and a source for $Re(b) > 0$. For $|a| = |b|$ one gets a whole line of zeros.

Proof : A computation of the derivatives of the components v_1, v_2 and a comparison with the classic classification gives this result. QED.

We included this theorem to show that this description gives topological information more directly. Let us look now at the general polynomial case

Theorem 6 . *Let $v : R^2 \rightarrow R^2 \subset G_2$ be an arbitrary polynomial vector field with isolated critical points. Let $E : C^2 \rightarrow C$ be the polynomial so that $v(r) = E(z,\bar{z})e_1$. Let $F_k : C^2 \rightarrow C$, $k = 1, \ldots, n$ be the irreducible components of E, so that $E(z,\bar{z}) = \prod_{k=1}^n F_k$. Then have the vector fields $w_k : R^2 \rightarrow R^2$, $w_k(r) = F_k(r)e_1$ also only isolated zeros $z_1, \ldots, z_m$. These are then the zeros of v and for the Poincaré-indices we have*

$$ind_{z_j} v = \sum_{k=1}^n ind_{z_j} w_k \tag{18}$$

Proof : See [Sche97b]. QED.

For experiments we use linear factors because of their behavior from Theorem 5.

Theorem 7 . *Let $v : R^2 \rightarrow R^2 \subset G_2$ be the vector field $v(r) = E(z,\bar{z})e_1$ with*

$$E(z,\bar{z}) = \prod_{k=1}^n (a_k z + b_k \bar{z} + c_k), \tag{19}$$

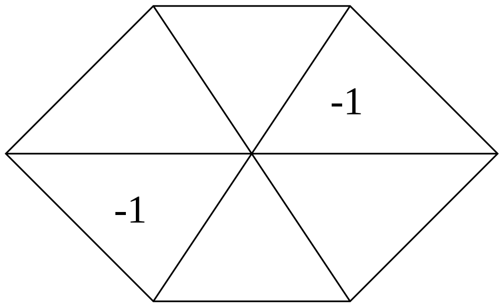

Figure 1: Indices of triangles around a triangle with two saddles

$|a_k| \neq |b_k|$ and let z_k be the unique zero of $a_k z + b_k \bar{z} + c_k$. Then has v zeros at z_j, $j = 1, \ldots, n$ and the Poincaré index of v at z_j is the sum of the indices of the $(a_k z + b_k \bar{z} + c_k)e_1$ at z_j.

Proof : Special case of Theorem 6 QED.

5 THE ALGORITHM

This section shows a way for the visualization of vector fields without topological restrictions coming from piecewise linear approaches.

Our central point is the fact that the distance between critical points in conventional approaches depends on the grid because each linear cell has usually only one critical point. In two dimensions there is an unstructured grid consisting of triangles. When we approximate the triangles by linear interpolation then each triangle contains only one critical point but in reality there may be more inside. The key for a solution is to analyse the data to get information about the number and index of critical points and to choose an approximation in the light of the theorems to allow several critical points. Outside the areas with more than one critical point we still use linear interpolation to keep the algorithm fast.

The basic idea is that a critical point has topological implications into the field if its Poincaré index is different from 0. In figure 1 there are two close saddles in one triangle, but in a piecewise linear approximation there will be two different triangles containing one saddle each.

This behavior tells how to find such situations. If several critical points are in the same cell and have the same index, there are close cells with critical points of that index in the linear approach. These areas are found in a first step and then one can approximate with polynomials like the ones in the last section. In our example above one could use

(20)
$$v(r) = (a_1 z + b_1 \bar{z} + c_1)(a_2 z + b_2 \bar{z} + c_2)e_1$$

in this area and then one can get the saddles in the same triangle.

Our algorithm includes the following steps :

(1) Compute the Poincaré index around each triangle assuming linear interpolation along the edges. One gets -1, 0 or +1.

(2) Build the regions of close triangles with possible higher order critical points.

   (a) If there are two triangles with a common edge and opposite index as in figure 2, mark them and save the neighboring connection.

   (b) If there are unmarked triangles with the same index and a common vertex, put all the triangles with that vertex in a region as in figure 3. If one of the triangles was marked in (a), put its neighbor also in the region as in figure 4. If any of the triangles is already in a region, do not build this region. Otherwise mark all the triangles in this new region.

   (c) If there are unmarked triangles A and B with the same index and a triangle C with a common edge with A and a common vertex V with B as in figure 5, build a region consisting of A and all the triangles having V as vertex. Like (b) look for triangles which have been marked in (a) and make sure to put the neighbors always also in the region. Again, if any triangle in this new region is already in a region, do not build this region.

(3) Compute the index of each region by just adding the index of all triangles in that region. Then set up a polynomial approximation of the type

$$v(r) \quad = \quad (a_1 z + b_1 \bar{z} + c_1) *$$

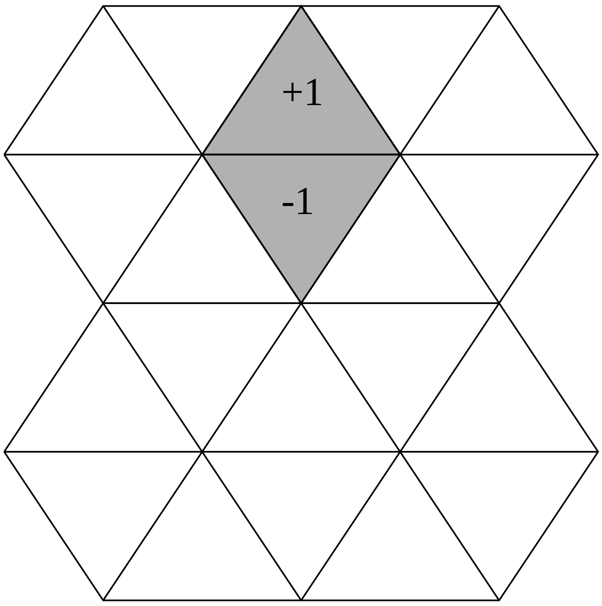

Figure 2: Triangles with opposite indices

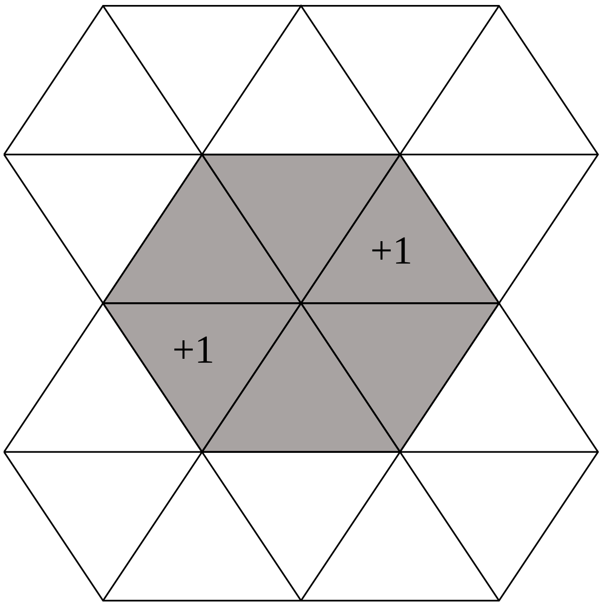

Figure 3: Triangles with opposite indices

$$(a_2 z + b_2 \bar{z} + c_2) * \cdots * (a_n z + b_n \bar{z} + c_n) e_1 \tag{21}$$

We are not maintaining continuity across the boundaries at the moment but are considering some kind of blending in an area close to the boundary of our regions to solve this problem.

The pictures on the final page show an example of the algorithm. It is applied to a field containing a monkey saddle, a dipole and several simple critical points on a 50×50 quadratic grid with coordinates $[-1, 1] \times [-1, 1]$. Figure 6 shows the piecewise linear approximation. The problem appears around the dipole and the monkey saddle where one has two critical points instead of one. Figure 7 contains a zoom into the interesting part around the monkey saddle. Figure 8 and 9 show the results obtained by using the new algorithm.

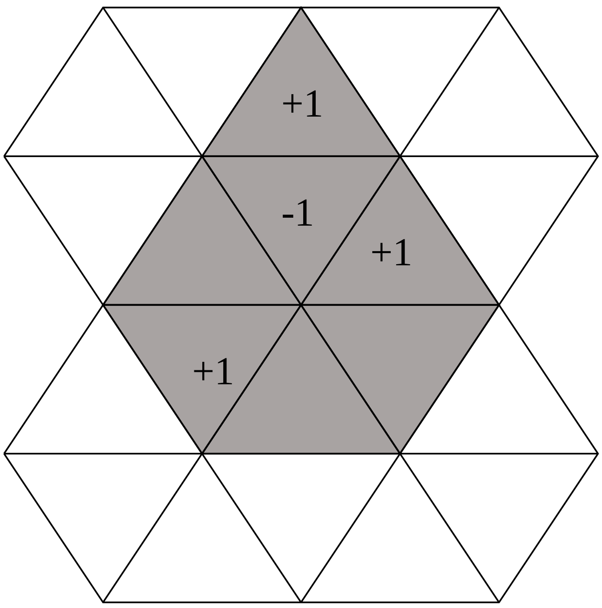

Figure 4: A +2-region with +1/-1-pair

6 ACKNOWLEDGEMENT

We want to thank Alan Rockwood, Greg Nielson and David Hestenes from Arizona State University for many comments, ideas and inspiration.

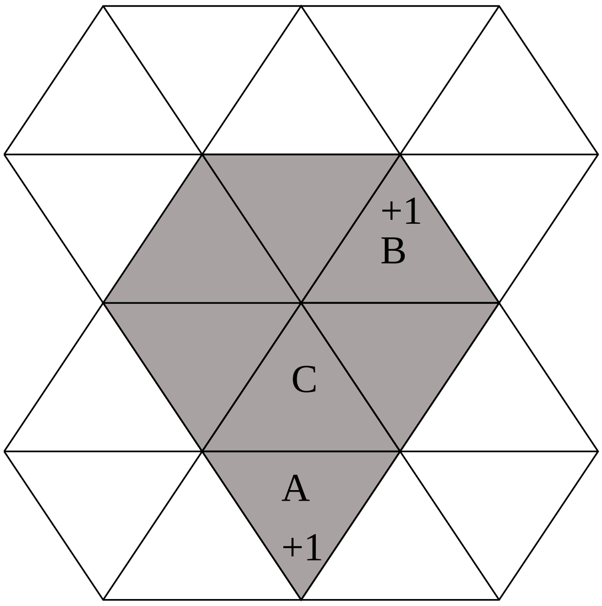

Figure 5: A more complicated region

References

[Arno91] Arnold, V. I.: *Gewöhnliche Differentialgleichungen*, Deutscher Verlag der Wissenschaften, Berlin, 1991.

[Glob91] Globus, A., Levit, C., Lasinski, T.: *A Tool for Visualizing the Topology of Three-Dimensional Vector Fields*, IEEE Visualization '91, Proc., pp. 33–40, 1991.

[Guck83] Guckenheimer, J., Holmes, P.: *Nonlinear Oszillations, Dynamical Systems and Bifurcations of Vector Fields*, Springer, New York, 1983.

[Helm91] Helman, J. L., Hesselink, L.: *Visualizing vector field topology in fluid flows*, IEEE Computer Graphics and Applications **11**:3 (1991), 36–46.

[Hest86] Hestenes, D.: *New Foundations for classical mechanics*, Kluwer Academic Publishers, Dordrecht, 1986.

[Hirs74] Hirsch, M. W., Smale, S.: *Differential Equations, Dynamical Systems and Linear Algebra*, Academic Press, New York 1974

[Krue96] Krüger, H., Menzel, M.: *Clifford-analytic vector fields as models for plane electric currents*, Analytical and Numerical Methods in Quaternionic and Clifford Analysis (W. Sprössig, K. Gürlebeck, eds.), Seiffen, 1996.

[Sche97a] Scheuermann, G., Hagen, H., Krüger, H., Rockwood, R.: *Examples of Clifford vector fields in two dimensions*, Technical Report, Arizona State University, 1997.

[Sche97b] Scheuermann, G., Hagen, H., Krüger, H., Menzel, M., Rockwood, R.: *Visualization of Higher Order Singularities in Vector Fields*, accepted for IEEE Visualization '97, Phoenix, 1997.

[Stoe94] Stoecker, R., Zieschang, H.: *Algebraische Topologie*, Teubner, Stuttgart, 1994.

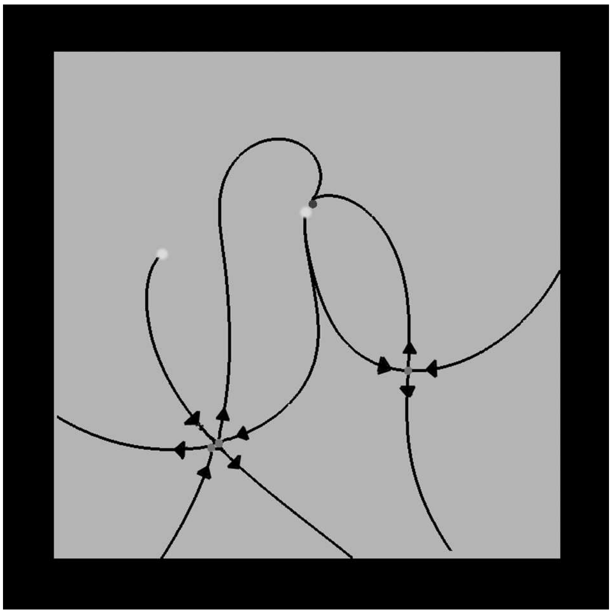

Figure 6: Linear approximation around monkey saddle

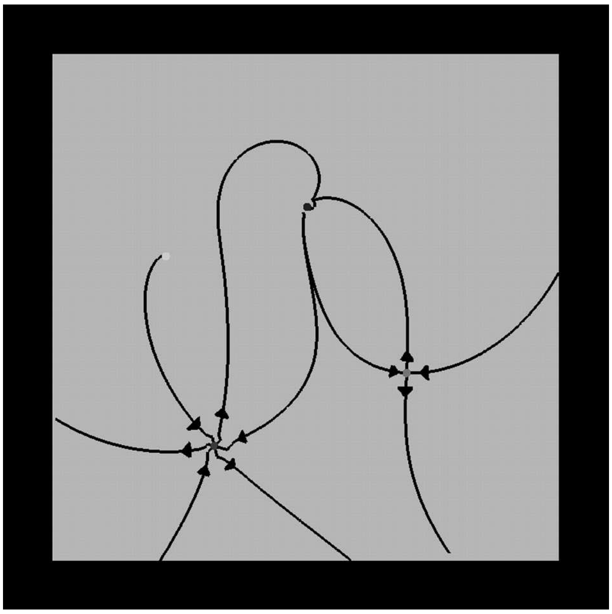

Figure 8: Clifford approximation around monkey saddle

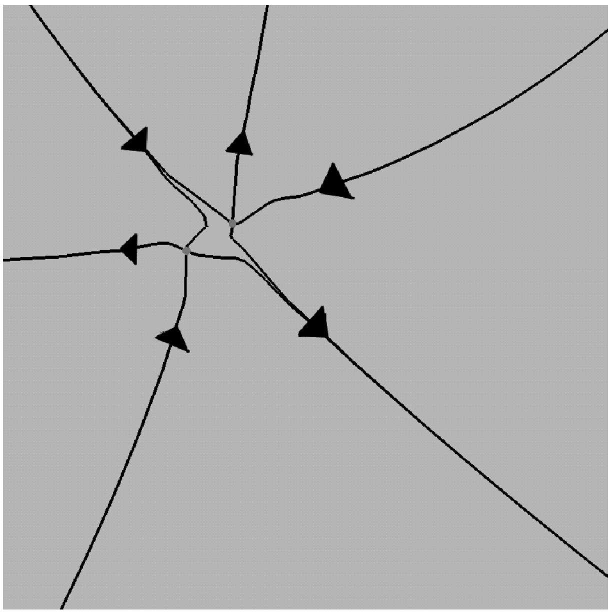

Figure 7: Zoom of linear approximation around monkey saddle

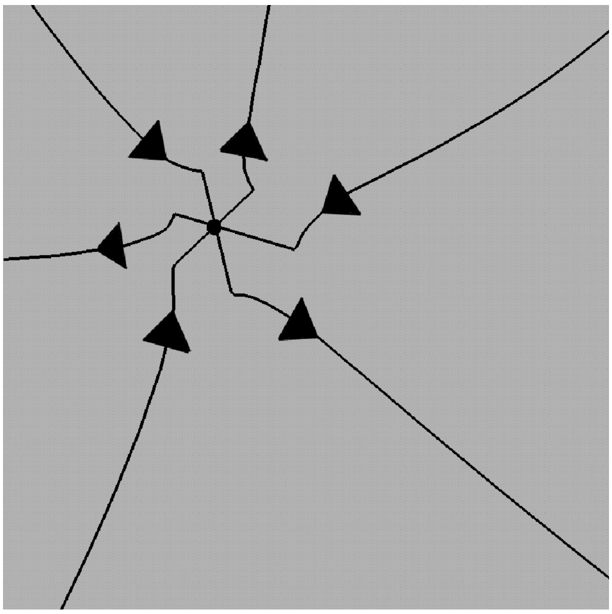

Figure 9: Zoom of Clifford approximation around monkey saddle